

FTIR Microspectroscopic Analysis of Human Iliac Crest Biopsies from Untreated Osteoporotic Bone

E. P. Paschalis,¹ F. Betts,¹ E. DiCarlo,¹ R. Mendelsohn,² A. L. Boskey¹

¹The Hospital for Special Surgery, 535 E. 70th St., New York, New York 10021, USA

²Chemistry Department, Rutgers University, Newark, New Jersey, USA

Abstract. Historically, osteoporosis has been defined as a disease in which there is “too little bone, but what there is, is normal.” As a result of research design and sample selection limitations, published data contradict and confirm the historical definition. Because of these limitations, it has been hard to assess the contribution of mineral quality to mechanical properties, and to select therapeutic protocols that optimize bone mineral properties. The coupling of an optical microscope to an infrared spectrometer enables the acquisition of spectral data at known sites in a histologic section of mineralized tissue without loss of topography and/or orientation. The use of second-derivative spectroscopy coupled with curve-fitting techniques allows the qualitative and quantitative assessment of mineral quality (crystallite size and perfection, mineral:matrix ratio) at well-defined morphologic locations.

We have previously applied these techniques to the study of normal human osteonal, cortical, and trabecular bone. The results indicated that the newly deposited bone mineral is less “crystalline/mature” than the older one. In the present study, Fourier transform infrared microspectroscopy (FTIRM) was applied to the study of human osteonal and cortical bone from iliac crest biopsies of untreated osteoporotic patients. The hypothesis tested was that osteoporotic bone mineral is monotonically different in its properties expressed as “crystallinity/maturity” than the normal. The results indicate significant differences in the mineral properties as expressed by crystal size and perfection, with the mineral from osteoporotic bone being more crystalline/mature than the normal.

Key words: Osteoporosis — Bone apatite — FTIR microspectroscopy — Osteon — Cortical bone.

Osteoporosis, defined by clinicians as decreased bone mass (osteopenia), sufficient to result in fractures with minimal trauma, is one of the major causes of death in women [1]. In the US, osteoporosis causes 1.3 million fractures per year [1], imposing a tremendous burden on the financing of health care [2]. Osteoporosis, most frequently encountered in postmenopausal women, is not a disease exclusive to women; it occurs, albeit to a lesser extent, in men [3] and in younger individuals [4]. Basic information is lacking on the etiologies of osteoporosis and the tissue changes that are

characteristic of the disease. Such information is necessary to understand the disease and develop effective therapies.

Osteoporosis was defined by Albright and Reifenstein [5] as a “disease in which there is too little bone, but what there is, is normal.” At least in terms of the mineral component, the literature on this subject is sparse and conflicting [6]. In both animal models and in humans it has been reported that osteoporotic bone mineral characteristically consists of crystals that are larger and more perfect than those in normal bone [7–10], smaller and less perfect [11], or that there are no differences [12]. Typically in these studies, tissues are homogenized prior to analysis thus concealing the effect of spatial variations in mineral properties.

The identity of the mineral is more often established by X-ray studies and electron diffraction, spectroscopic means (e.g., Raman, IR, FTIR), and nuclear magnetic resonance (NMR), each of which requires homogenized tissues [13–18]. Because mineral properties vary spatially and temporally, Fourier transform infrared microspectroscopy (FTIRM) analysis has been successfully applied to the study of changes in mineral properties with a spatial resolution of 20 μm in histological sections of mineralized tissues [19–23]. This technique has recently been placed on a quantitative basis relating data obtained by a combination of derivative spectral parameters and curve-fitting, with “crystallinity/maturity/perfection,” a parameter dependent on crystallite size, hydroxyapatite-like stoichiometry, and abundance of substituting ions such as CO_3^{2-} ; the more “crystalline/mature,” the more hydroxyapatite-like stoichiometry, the bigger the crystallite size, the less the ion substitution by ions such as CO_3^{2-} [23–25].

We have previously stated that there are reproducible changes in the mineral of normal bone that are related to anatomical topography and bone age [23, 25]. The purpose of the current study was to test the hypothesis that osteoporotic bone mineral is different from normal by comparing spatial variations in spectral parameters observed in iliac crest biopsies from normal and untreated osteoporotic patients. In the current work, attention is focused on the ν_1 , ν_3 phosphate band contour (900–1200 cm^{-1}) as it is readily accessible in studies of mineralized tissues using FTIRM with a Mercury-Cadmium-Telluride detector. Qualitative and quantitative variations in the broad FTIR contours of biologic apatites were determined by second-derivative spectroscopy (to resolve the underlying bands) and curve-fitting analysis (to quantitate the contribution of the underlying bands). The results indicate that in general, mineral in osteoporotic bones exhibits higher crystallinity/maturity in the anatomical area of newly deposited bone (osteonic center, periosteum) than normal bone.

Table 1. Summary of the various patients and results of their biopsy studies

Age (years)	Sex	Comments
65	Male	Normal N1
55	Male	Normal N2
53	Female	Low turnover osteoporosis with decreased formative activity, and increased resorptive surface, inactive. Long-term steroid-dependent rheumatoid arthritis (A)
41	Male	Osteoporosis with decreased formative activity and increased resorptive surface, active (B)
31	Female	Osteoporosis with increased formative activity and increased resorptive surface, active. Borderline anorexic-avid long-distance runner (C)

A, B, C: Patients with osteoporotic bone

Materials and Methods

Iliac crest biopsy specimens from untreated osteoporotic patients with different pathologies were analyzed and compared with normal biopsy data previously reported [23, 25]. Table 1 is a summary of the patients and results of their various biopsies. The tissues were fixed in 70% ethanol, dehydrated through serial acetones, embedded in polymethyl methacrylate (PMMA), and cut into 5 μm -thick sections using a Jung Model K microtome (Reichert-Jung, Heidelberg, Germany). The PMMA was subsequently removed by soaking the sections in methyl acetate or acetone, followed by washing with methanol to remove any residue. They were then transferred onto BaF₂ windows, covered with a second window to avoid any rippling of the section, and analyzed by FTIR microspectroscopy. Spectra were recorded with a UMA 500 microscope with a motorized xy stage, coupled to an FTS-40 spectrometer (both from Bio-Rad Inc., Cambridge, MA), at a resolution of 4 cm^{-1} , 1024 scans, in the transmission mode. A Screen Image Recorder (AVIO, Japan) camera was also attached to the microscope, enabling the acquisition of photomicrographs from the area of analysis. The area of each spectroscopic analysis was $20 \times 20 \mu\text{m}^2$. Sequential spectra were recorded at predetermined intervals by the motorized microscope stage. In the area of the osteons, spectra were recorded as described previously [23] in 10- μm steps, originating at the osteonal center [23]. The results of all osteons examined for each patient were averaged with standard deviation (SD) plotted as error bars. In the cortical bone, spectra were obtained across (in steps of 125 μm) the lamellae, in areas devoid of visible osteons and osteocytes [25]. This analysis was performed in triplicate sections, the resulting values averaged, and standard deviation plotted as error bars.

Trabecular bone could not be analyzed in osteoporotic samples because when PMMA was removed the integrity of the sparse trabecular bone was not retained. Consequently, only the cortices from the iliac crest biopsies were analyzed. At the conclusion of these analyses, the sections were treated with a 5% EDTA solution in order to decalcify them, and spectra were recorded at identical positions with the previous undecalcified set. The purpose of this second group of spectra was to provide a reference set of data for spectral subtraction of the organic matrix contribution to the mineral spectra. Water vapor was also spectrally subtracted from the initial spectra. After this, the region 800–1750 cm^{-1} was baseline corrected, and mineral:matrix ratios were obtained by integrating the area under the peaks at 900–1200 cm^{-1} (phosphate) and ≈ 1590 –1700 cm^{-1} (Amide I). Second-derivative spectra were calculated in the ν_1 , ν_3 phosphate region (900–1200 cm^{-1}) in an effort to isolate the underlying peaks that constitute the broad, relatively featureless contour of this peak. A more detailed discussion of this technique is given elsewhere [22–25]. The peak positions in the second-derivative spectra were recorded and utilized as initial in-

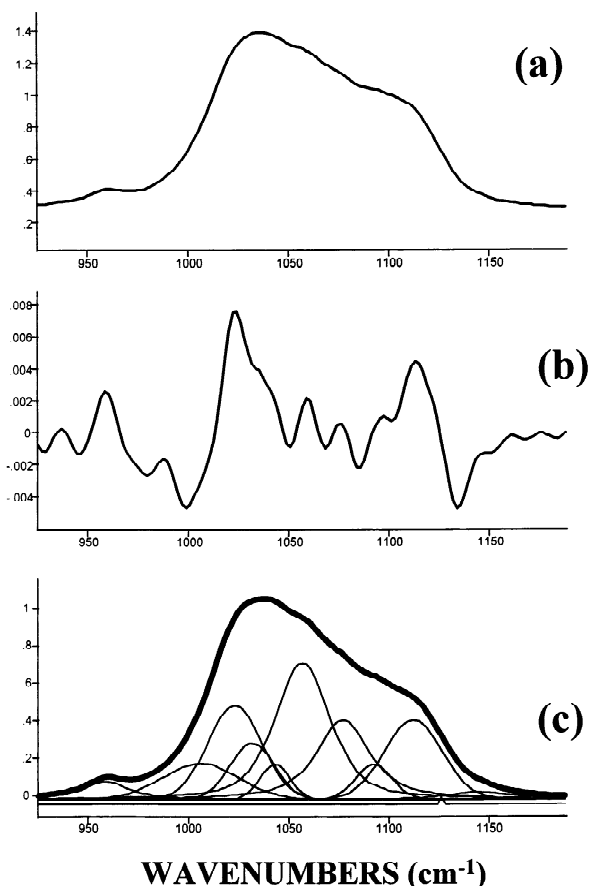


Fig. 1. Typical raw absorbance FTIRM spectrum obtained in the area of primary cortical bone in a section from a biopsy from patient A (a), its calculated second-derivative spectrum resolving the position of the various underlying bands (b), and the resulting underlying bands deduced by curve-fitting analysis (c).

put in a commercially available curve-fitting software package (gs/386, Galactic Industries Corporation, Salem, NH, USA). The output of this analysis was expressed as relative peak area and peak position. Of the resulting underlying peaks, the ones at $\approx 1020 \text{ cm}^{-1}$ and $\approx 1030 \text{ cm}^{-1}$ were used to assess mineral crystallinity/maturity. These two subbands have been assigned in the literature as indicative of nonstoichiometric/substituted and stoichiometric apatites, respectively [26]. The ratio of the relative areas of these two peaks has been previously shown to provide a sensitive and reproducible index of crystal size and perfection [23, 25].

All the values that were obtained from the various measurements were subjected to statistical analysis for linear trend, non-linear variation, and Dunnett multiple comparisons test, with the values of normal bone serving as the control using a commercially available statistical package (GraphPad InStat 2.01, GraphPad Software).

Results

Figure 1 shows a typical FTIR absorbance spectrum of an untreated osteoporotic human iliac crest biopsy in the ν_1 , ν_3 phosphate region (a), its calculated second-derivative spectrum (b), and the results of curve-fitting analysis on this spectrum showing the underlying bands (c). The relative mineral:matrix ratio was calculated from the raw spectra by integrating the appropriate peaks.

Figure 2 is a composite of the mineral:matrix ratio cal-

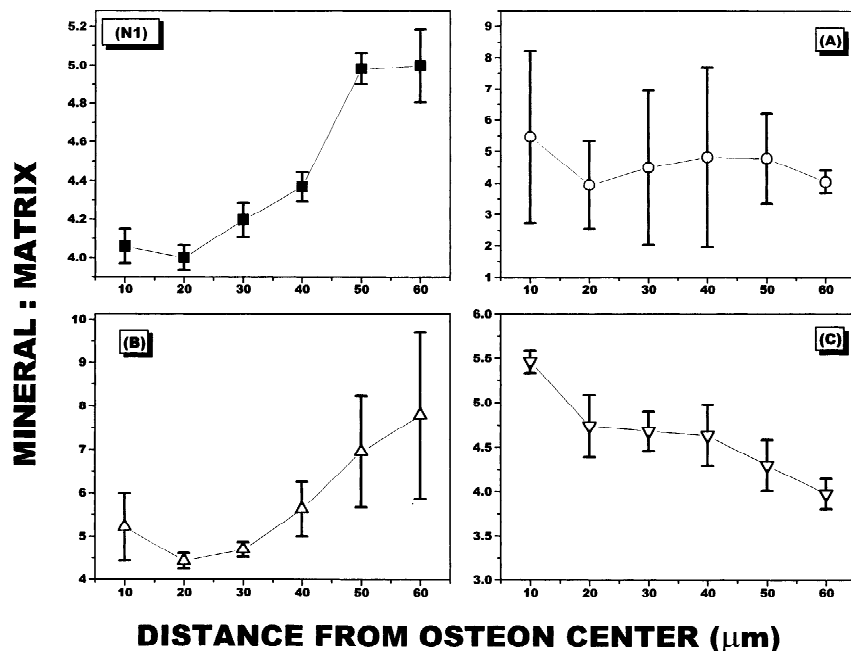


Fig. 2. Relative mineral content expressed as mineral:matrix ratio obtained from the ratio of the integrated PO_4^{3-} and Amide I peaks. The analysis was performed in the area of osteons, as a function of distance from the osteonal center (haversian canal). N1 = normal bone. See **Results** for (A), (B), and (C).

culated in the areas of osteons for normal (N1) and osteoporotic bone (A, B, C). These values were determined every 10 μm starting in the osteonal center and going towards its periphery, and they were plotted as a function of anatomical position. The values for the normal bone show both a significant linear trend ($P < 0.0001$) as well as variance among each other ($P = 0.0198$). For the 53-year-old female osteoporotic patient (A), this ratio showed neither a significant linear trend ($P = 0.4822$) nor significant variance among the calculated mean values ($P = 0.6453$). In the case of the 41-year old male (B), the calculated mineral:matrix values as a function of distance from the osteonal center showed a significant linear trend ($P = 0.0138$), a greater range of values than seen in N1, but no significant variance among the calculated mean values ($P = 0.7160$). Similarly, the corresponding data obtained from the analysis of iliac crest biopsies from the 39-year-old female (C) also show a statistically significant linear trend ($P < 0.0001$), but values tended to decrease rather than increase as in the normal, and there was no significant variance ($P = 0.7307$).

We have previously shown that the relative ratio of the underlying bands at 1020 and 1030 cm^{-1} provides an indication of mineral crystallinity/maturity [23, 25]. The spectra acquired from all patients in the area of osteons were curve fit and the 1020/1030 ratio was calculated as function of distance from the osteonal center. Figure 3 is a composite graph of this parameter for all the cases examined in this study. In the case of normal osteonal bone (N1) this ratio showed a significant linear trend ($P < 0.0001$) and variation among the calculated means ($P < 0.0001$). When this ratio was deduced from spectra obtained in osteons from the 53-year-old osteoporotic female (A), there was neither a significant linear trend ($P = 0.1986$) nor variability ($P = 0.0741$). For the case of the 41-year-old osteoporotic male (B), the 1020/1030 ratio showed a significant linear trend ($P < 0.0001$), but not significant variability ($P = 0.8731$). Finally, the calculated 1020/1030 ratio for the spectra obtained from the 31-year-old osteoporotic female (C) behaved as in the case of normal bone, displaying both sig-

nificant linear trend ($P < 0.0001$) and variability ($P = 0.0016$).

The calculated values for the parameters reported in this paper, i.e., mineral:matrix ratio, and 1020/1030 peak area ratios, were compared with the normal data at equivalent anatomical positions (distance from the osteonal center). Dunnett's multiple comparisons test was used for statistical analysis. No variations in mineral:matrix ratio was found (Table 2), but there were significant differences in crystallinity/maturity in the most recently deposited mineral in the osteon (Table 3).

The various biopsies were also analyzed in the area of the cortical bone, with the line of analysis proceeding from the periosteal bone (low x-values) towards the medullary cavity (higher x-values). The same parameters as the ones previously reported were determined and are shown in Figure 4 (mineral:matrix) and Figure 5 (1020/1030). Each figure is a composite graph of the individual plots with the values obtained for each case used in the present study. For each case, three lines of analysis were considered, the obtained values were averaged, and SD was reported as error bars. Caution was exercised so that the lines of analysis did not pass through any visible osteons/osteocytes so as to avoid the extra variability [23, 25]. These values were compared among each other at equivalent anatomical positions with the values of normal bone serving as the control. As in the case of osteonal bone, there were no significant differences between normal and osteoporotic bone when mineral:matrix ratios were compared (Table 4). On the other hand, only the newest formed bone showed significant variation in mineral crystallinity/maturity from normal controls (Table 5).

Discussion

This study presents for the first time confirmation of the variability in the mineral properties seen in osteoporotic bone. Earlier studies using homogenized tissues had reported that the crystallinity (crystal size and perfection) in

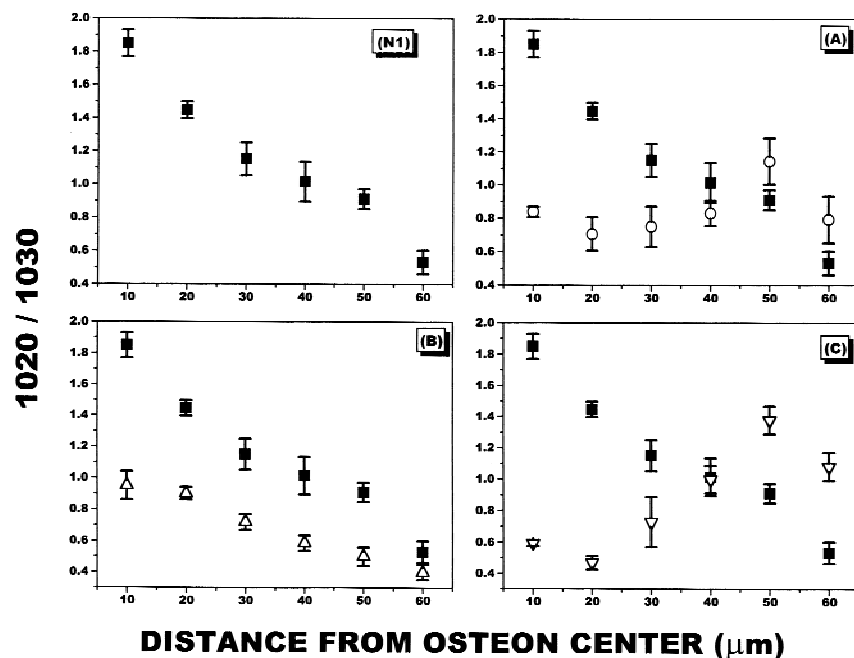


Fig. 3. Typical results of the calculated 1020/1030 ratios in the area of osteons, as a function of distance from the osteonal center (haversian canal). This ratio is inversely proportional to crystal perfection/maturation.

Table 2. Comparison of mineral:matrix ratios between normal and osteoporotic cases in the area of osteons at equivalent anatomical positions

Distance from osteon center (μm)	N1 vs A	N1 vs B	N1 vs C
10	$P > 0.05^a$	$P > 0.05$	$P > 0.05$
20	$P > 0.05$	$P > 0.05$	$P > 0.05$
30	$P > 0.05$	$P > 0.05$	$P > 0.05$
40	$P > 0.05$	$P > 0.05$	$P > 0.05$
50	$P > 0.05$	$P > 0.05$	$P > 0.05$
60	$P > 0.05$	$P > 0.05$	$P > 0.05$

All probabilities (P) not significantly different

Table 3. Comparison of 1020/1030 ratios between normal and osteoporotic cases in the area of osteons, at equivalent anatomical positions

Distance from osteon center (μm)	N1 vs A	N1 vs B	N1 vs C
10	$P < 0.01^c$	$P < 0.01^c$	$P < 0.01^c$
20	$P < 0.01^c$	$P < 0.01^c$	$P < 0.01^c$
30	$P < 0.05^b$	$P < 0.05^b$	$P < 0.05^b$
40	$P > 0.05^a$	$P < 0.01^c$	$P > 0.05^a$
50	$P > 0.05^a$	$P < 0.01^c$	$P < 0.01^c$
60	$P > 0.05^a$	$P > 0.05^a$	$P < 0.01^a$

^a Not significantly different

^b Different

^c Significantly different

osteoporotic bone was decreased [11], increased [7–10], or invariant [12]. This initial study using a range of osteoporotic tissues reveals that the reproducible anatomic variation in mineral properties seen in normal bones is not found in osteoporosis.

A major difficulty associated with analysis of bone is tissue heterogeneity. Malluche and others [27–29] have demonstrated through histomorphometry that a series of iliac crest biopsies taken from a single cadaver bone can show evidence of marked osteopenia, severe osteomalacia, or no bone disease. However, when trends in individual osteons are compared in multiple (as many as 16) biopsies in the same individual, anatomic variations are reproducible [23, 25]. When these trends are used as a “baseline” against which osteoporotic bone is compared, reproducible differences between normal and osteoporotic bone emerge in that the osteoporotic bone invariably exhibits higher crystallinity/maturity than normal in the anatomical regions of osteons and periosteal bone.

Patient A is a low-turnover osteoporosis case, with long-term steroid-dependent rheumatoid arthritis. The results of mineral:matrix ratio and 1020/1030 ratios indicate absence

of “young” bone, which may be a reflection of the steroid treatment. Patient B exhibits a similar mineral:matrix ratio profile as the normal (N1). Yet the 1020/1030 ratio in the area of osteons reveals that the mineral is more crystalline/mature than normal. These observations may be attributable to the decreased formative activity and increased resorptive surface that the patient was diagnosed with, in that the slow bone formation favors the maturation of the existing mineral, while the small bone crystallites are dissolved rapidly due to the increased resorption. Finally, patient C also exhibits more mature bone crystals than normal, but the case is complicated even further by the fact that she is borderline anorexic and an avid long-distance runner.

FTIRM offers the unique advantage that the bone mineral in thin sections may be analyzed without prior homogenization of the sample, thus routinely providing data at a spatial resolution of 20 μm. This feature allows for the correlation of mineral properties with specific anatomic “landmarks” such as osteons. The disadvantage associated with this technique is that, due to detector limitations, only the ν_1 , ν_3 PO_4^{3-} spectral region (900–1200 cm^{-1}) is acces-

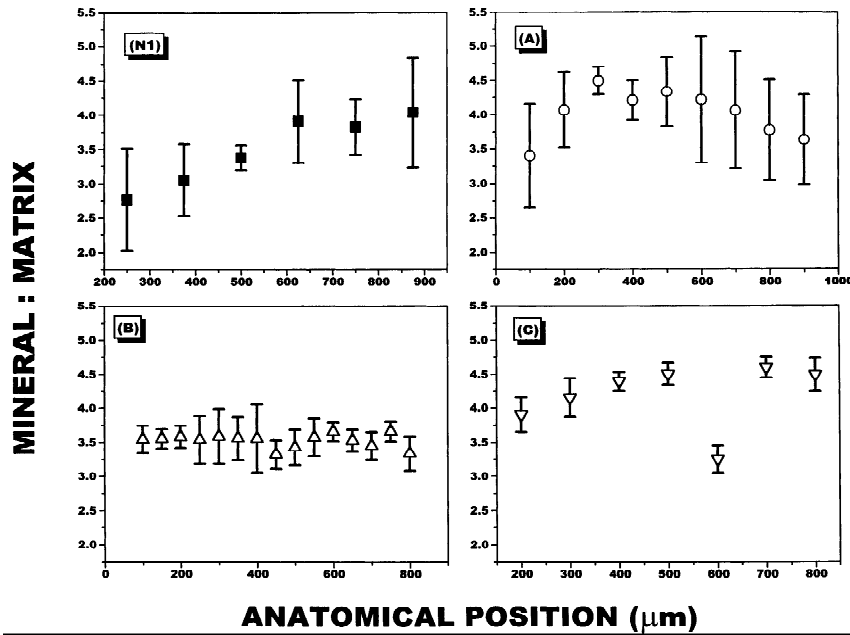


Fig. 4. Relative mineral content expressed as mineral:matrix ratio obtained from the ratio of the integrated PO_4^{3-} and Amide I peaks. The analysis was performed in the primary cortical bone area, commencing at the periosteal and proceeding towards the endosteal side.

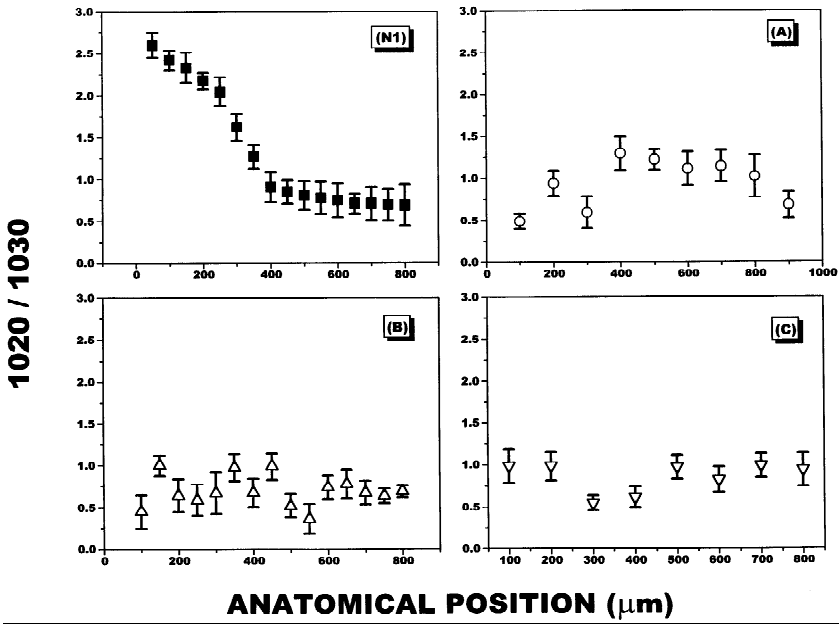


Fig. 5. Calculated 1020/1030 ratios in the area of primary cortical bone, as a function of distance from the periosteal end.

Table 4. Comparison of mineral:matrix ratios between normal and osteoporotic cases in the cortical bone at equivalent anatomical positions

Anatomical position (μm)	N1 vs A	N1 vs B	N1 vs C
200	$P > 0.05$	$P > 0.05$	$P > 0.05$
400	$P > 0.05$	$P > 0.05$	$P > 0.05$
600	$P > 0.05$	$P > 0.05$	$P > 0.05$
800	$P > 0.05$	$P > 0.05$	$P > 0.05$

All probabilities: (P) not significantly different

Table 5. Comparison of 1020/1030 ratios between normal and osteoporotic cases in the cortical bone at equivalent anatomical positions

Anatomical position (μ)	N1 vs A	N1 vs B	N1 vs C
200	$P < 0.01^a$	$P < 0.01^a$	$P < 0.01^a$
400	$P > 0.05$	$P > 0.05$	$P > 0.05$
600	$P > 0.05$	$P > 0.05$	$P > 0.05$
800	$P > 0.05$	$P > 0.05$	$P > 0.05$

Probabilities (P) not significantly different

^aProbabilities significantly different

sible. This contour is a broad composite of underlying bands, each specifically describing certain phosphate environments. Through second-derivative spectroscopy and curve-fitting analysis these bands may be resolved, thus permitting mineral properties such as crystallinity/maturity to be reproducibly assessed. Although the differences between normal and osteoporotic bone presented in this study were reproducible and independent of the type of osteoporosis, the data should be verified by examining multiple patients for each type.

Recently, osteoporosis was defined as "a disease characterized by low bone mass and microarchitectural deterioration of bone tissue, leading to enhanced bone fragility and a consequent increase in fracture risk" [30, 31]. Working definitions of osteoporosis are based exclusively on bone mass [32]. Such definitions are of great importance in the clinical field, but do not provide information about either the nature and causes of osteoporosis or the quality of bone mineral that remains. On the other hand, FTIRM analysis of normal and osteoporotic bone established that in the areas that normal bone manifests the presence of "young"/immature mineral (osteonal center, periosteal bone), the osteoporotic bone mineral exhibits higher crystallinity/maturity.

In conclusion, employing FTIRM analysis of thin sections obtained from iliac crest biopsies, the present report is the first to establish consistent differences among normal and osteoporotic human bone mineral. Osteoporotic bone invariably exhibited bigger mineral crystallinity/maturity than normal samples in the area of osteons and periosteal bone. This difference is likely to negatively affect the mechanical properties of the osteoporotic bone. In this paper we established the reproducibility of these differences. Examination of biopsies from more osteoporotic patients should clarify whether this technique may be of diagnostic value. Furthermore, it should be noted that the present results were obtained by examining the area of the ilium, and may or may not necessarily extrapolate to the situation in the trabecular bone.

Acknowledgments. This work was supported by NIH Grant #AR41325.

References

- Jensen KS, Mosekilde L (1990) A model of vertebral trabecular bone architecture and its mechanical properties. *Bone* 11:417–423
- Simonen O (1986) Osteoporosis: a big challenge to public health. *Calcif Tissue Int* 39:295–296
- Foldes I, Rapcsak M, Szilagyi T, Oganov VS (1990) Effects of space flight on bone formation and resorption. *Acta Physiol Hung* 75:271–285
- Barschach LK, Guido D, Katzman D, Litt IF, Marcus R (1990) Decreased bone density in adolescent girls with anorexia nervosa. *Pediatrics* 86:440–447
- Albright F, Reifenstein EC (1948) The parathyroid glands and metabolic bone disease. Williams and Wilkins, Baltimore, MD, p 393
- Boskey AL (1990) Bone mineral and matrix: Are they altered in osteoporosis? *Orthop Clin North Am* 21:19–29
- Baud CA, Pouezat JA, Tocho-Danguy HJ (1976) Quantitative analysis of amorphous and crystalline bone tissue mineral in women with osteoporosis. *Calcif Tissue Int* 21S:452–456
- Chatterji S, Wall JC, Jeffrey JW (1981) Age-related changes in the orientation and particle size of the mineral phase in human cortical bone. *Calcif Tissue Int* 33:577
- Ferris BB, Dodds C, Klenerman L (1987) Major components of bone in subcapital and trochanteric fractures. A comparative study. *J. Bone Joint Surg* 69B:234
- Rai DV, Behar J (1986) Biophysical characterization of osteoporotic bone. *Environ Res* 40:68
- Grynepas MD, Holmyard D (1988) Changes in quality of bone mineral on aging and in disease. *SEM* 2:1045–1051
- Grynpass MD, Katz I, Pritzker KPH (1987) Bone quality and bone quantity in osteoporosis. In: Christiansen C, Johansen JS, Riisi BJ (eds) *Osteoporosis, I*. Osteopress, Copenhagen, p 364
- Hukins DWL (1989) In: *Calcified tissue*, CRC Press,
- McCarty DJ, Lehr JR, Halverson PB (1983) Crystal populations in human synovial fluid. Identification of apatite, octacalcium phosphate, and tricalcium phosphate. *Arthritis Rheum* 26:1220–1224
- Sauer GR, Zunic WB, Durig JR, Wuthier RE (1994) Fourier transform Raman spectroscopy of synthetic and biological calcium phosphates. *Calcif Tissue Int* 54:414–420
- Sauer GR, Wuthier RE (1988) Fourier transform infrared characterization of mineral phases formed during induction of mineralization by collagenase-released matrix vesicles in vitro. *J Biol Chem* 263:13718
- Satomura K, Hiraiwa K, Nagayama M (1991) Mineralized nodule formation in rat bone marrow stromal cell culture without beta-glycerophosphate. *Bone Miner* 14:41–54
- Derfus BA, Rachow JW, Mandel NS, Boskey AL, Buday M, Kushnaryov VM, Ryan LM (1992) Articular cartilage vesicles generate calcium pyrophosphate dihydrate-like crystals in vitro. *Arthritis Rheum* 35:231–240
- Mendelsohn R, Hasankhani A, DiCarlo E, Boskey AL (1989) FT-IR microscopy of endochondral ossification at 20 μ m spatial resolution. *Calcif Tissue Int* 44:20–29
- Pleshko N, Boskey AL, Mendelsohn R (1992) An FT-IR microscopic investigation of the effects of tissue preservation on bone. *Calcif Tissue Int* 51:72–77
- Pleshko N, Boskey AL, Mendelsohn R (1992) An infrared study of the interaction of polymethyl methacrylate with the protein and mineral components of bone. *J Histochem Cytochem* 40:1413–1417
- Paschalis EP, Jacenko O, Olsen BR, Mendelsohn R, Boskey AL (1996) FT-IR microspectroscopic analysis identifies alterations in mineral properties in bones from mice transgenic for type X collagen. *Bone* 19–2
- Paschalis EP, DiCarlo E, Betts F, Sherman P, Mendelsohn R, Boskey AL (1996) FTIR microspectroscopic analysis of normal human osteonal bone. *Calcif Tissue Int* 59:480–487
- Gadaleta SJ, Paschalis EP, Betts F, Mendelsohn R, Boskey AL (1996) New infrared spectra structure correlations in the amorphous calcium phosphate to hydroxyapatite conversion. *Calcif Tissue Int* 58:9–16
- Paschalis EP, DiCarlo E, Betts F, Mendelsohn R, Boskey AL (1997) FTIR microspectroscopic analysis of normal human cortical and trabecular bone. *Calcif Tissue Int* (in press)
- Rey C, Shimizu M, Collins B, Glimcher MJ (1990) Resolution-enhanced fourier transform infrared spectroscopy study of the environment of phosphate ions in the early deposits of a solid phase of calcium-phosphate in bone and enamel, and their evolution with age. II: investigations in the ν_3 domain. *Calcif Tissue Int* 46:384–394
- Malluche HH, Meyer W, Sherman D (1982) Quantitative bone histology in 84 normal American subjects. Micromorphometric analyses and evaluation of variation in iliac bone. *Calcif Tissue Int* 34:449–455
- Ninonmiya JT, Tracy RP, Calore JD, Gendreau MA, Kelm RJ, Mann KG (1990) Heterogeneity of human bone. *J Bone Miner Res* 5:933–935
- Bonucci E, Ballanti P, Della Roca C (1990) Technical variability of bone histomorphometric measurements. *Bone Miner* 11:177–186
- Consensus Development Conference (1991) Prophylaxis and treatment of osteoporosis. *Am J Med* 90:107–110
- Consensus Development Conference (1993) Prophylaxis and treatment of osteoporosis. *Am J Med* 94:646–650
- Kanis JA, Melton LJ III, Christiansen C, Johnston C Jr, Haltaev N (1994) Perspective: the diagnosis of osteoporosis. *J Bone Miner Res* 9:1137–1142